Hindawi
International Journal of Antennas and Propagation
Volume 2019, Article ID 8094908, 13 pages
https://doi.org/10.1155/2019/8094908

*Research Article*

# Triband Compact Printed Antenna for 2.4/3.5/5 GHz WLAN/WiMAX Applications

**Pracha Osklang**[1], **Chuwong Phongcharoenpanich**[2] **and Prayoot Akkaraekthalin**[3]

[1]*Electronics and Telecommunication Technical Education, Rajamangala University of Technology Isan, Khonkaen Campus, Khonkaen, Thailand*
[2]*Faculty of Engineering, King Mongkut's Institute of Technology Ladkrabang, Bangkok, Thailand*
[3]*Department of Electrical and Computer Engineering, Faculty of Engineering, King Mongkut's University of Technology North Bangkok, Bangkok, Thailand*

Correspondence should be addressed to Pracha Osklang; pracha.os@rmuti.ac.th

Received 21 December 2018; Revised 5 June 2019; Accepted 18 June 2019; Published 28 August 2019

Academic Editor: Jaume Anguera



This research presents a triband compact printed antenna for WLAN and WiMAX applications. The antenna structure consists of a folded open stub, long and short L-shaped strips, and asymmetric trapezoid ground plane. Besides, it is of simple structure and operable in 2.4 GHz and 5 GHz (5.2/5.8 GHz) WLAN and 3.5/5.5 GHz WiMAX bands. The folded open stub and long and short L-shaped strips realize impedance matching at 2.4, 3.5, 5.2, and 5.8 GHz, and the asymmetric trapezoid ground plane fine-tunes impedance matching at 5.2, 5.5, and 5.8 GHz. In addition, the equivalent circuit model consolidated into lumped elements is also presented to explain its impedance matching characteristics. In this study, simulations were carried out, and a prototype antenna was fabricated and experimented. The simulation and experimental results are in good agreement. Specifically, the simulated and experimental radiation patterns are omnidirectional at 2.4, 3.5, and 5.2 GHz and near-omnidirectional at 5.5 and 5.8 GHz. Furthermore, the simulated and measured antenna gains are 1.269–3.074 dBi and 1.10–2.80 dBi, respectively. Essentially, the triband compact printed antenna covers 2.4 GHz and 5 GHz (5.2/5.8 GHz) WLAN and 3.5/5.5 GHz WiMAX frequency bands and thereby is a good candidate for WLAN/WiMAX applications.

## 1. Introduction

Recent decades have witnessed increased adoption of wireless communications technologies in a wide variety of applications, including laptop computers, mobile phones, and portable devices. The phenomenon contributes to a rise in demand for compact multiband antennas.

In [1–5], dual-band antennas covering 2.4/5.2/5.8 GHz bands were proposed for wireless local area network (WLAN) applications. In [6–24], attempts were made to develop antennas for WLAN/WiMAX applications, including $\pi$-shaped slotted microstrip antennas with aperture-coupled feed [6], resonator antennas [7–9], dual and multipolarized antennas [10–12], magnetoelectric and magnetic dipole antennas [13, 14], frequency-reconfigurable antennas using PIN-diode switch [15–18], metamaterial antennas [19–21], antennas with inverted-L-shaped radiating elements and parasitic elements in the ground plane [22], antennas with pentagonal ring slot fed at the vertex and E-slip with backfeeding [23], and antenna with bow-tie slot in a single metal sheet on top of the flexible substrate [24]. However, these antennas fail to cover the entire WLAN frequency band (2.4/5.2/5.8 GHz).

As a consequence, various techniques have been proposed to further improve antenna coverage encompassing 2.4/5.2/5.8 GHz WLAN and 3.5/5.5 WiMAX bands [25–31], including a rectangular ring and a S-shaped strip connected to the feedline with a crooked U-shaped strip and three straight strips on back side [25], a microstrip-fed slot with a complimentary stub on a single dielectric medium [26], a V-shaped patch with a rectangular strip on top layer fed by a buried rectangular strip in the middle layer by proximity coupling [27], three strips for radiating elements [28], an

asymmetric coplanar strip with a reverse G-shaped slot and a U-shaped open stub [29], two inverted-L slots etched on the radiator [30], a small inner rectangular ring and an outer rectangular loop with three slits and double rings and a parasitic strip [31]. Although these antennas could cover 2.4/5.2/5.8 GHz WLAN and 3.5/5.5 GHz WiMAX bands, they suffer from bulkiness and fabrication complexity. In contrast, the proposed triband antenna of this research is compact and of simple structure. Besides, it can efficiently cover 2.4/5.2/5.8 GHz WLAN and 3.5/5.5 GHz WiMAX bands. Table 1 summarizes the aforementioned WLAN/WiMAX antennas and dimensions.

Specifically, this research proposes a WLAN/WiMAX triband compact printed antenna operable in 2.4 GHz and 5 GHz (5.2/5.8 GHz) WLAN and 3.5/5.5 GHz WiMAX bands. The antenna structure consists of a folded open stub, long and short L-shaped strips, and asymmetric trapezoid ground plane. In the study, simulations were carried out using computer simulation technology (CST) microwave studio, and experiments were undertaken using a fabricated prototype antenna. The simulation and experimental results are in good agreement, validating the suitability of the proposed triband antenna for WLAN and WiMAX applications.

The organization of this research is as follows: Section 1 is the introduction. Section 2 details the antenna structure, Section 3 includes the design principle and parametric study, and Section 4 discusses the experimental results and compares simulation and experimental results. The concluding remarks are provided in Section 5.

Table 1: Comparison between the existing WLAN/WiMAX antennas and the proposed triband antenna.

| Reference | Antenna size (mm) | WLAN (GHz) | WiMAX (GHz) |
|---|---|---|---|
| [6] | $60 \times 60 \times 11.58$ | 2.4 | 2.5/3.5 |
| [7] | $33 \times 36.4 \times 0.508$ | 1.8/2.45/5.2 | 3.5 |
| [8] | $40 \times 40 \times 1.6$ | 5.2/5.8 | 2.3/3.3/5.5 |
| [9] | $30 \times 34 \times 0.76$ | 2.4/5.2 | 3.5 |
| [10] | $40 \times 30 \times 0.79$ | 2.4/5.8 | 2.5/5.5 |
| [11] | $50 \times 50 \times 1.6$ | 2.1 | 3.5/5.5 |
| [12] | $35 \times 45 \times 1.5$ | 2.4/5.8 | 2.3/3.5/5.5 |
| [13] | $80 \times 65 \times 0.78$ | 2.4 | 2.5/3.5 |
| [14] | $40 \times 40 \times 0.764$ | 5.8 | 3.5 |
| [15] | $30 \times 20 \times 0.8$ | 2.45/5.7 | 3.5 |
| [16] | $50 \times 45 \times 1.6$ | 2.4/5.8 | 3.5 |
| [17] | $59 \times 31 \times 0.1$ | 2.4 | 3.5 |
| [18] | $45 \times 50 \times 1$ | 2.4 | 3.5/5.5 |
| [19] | $70 \times 44 \times 1.6$ | 2.4/5.8 | 2.5/5.5 |
| [20] | $35 \times 38 \times 1$ | 5.8 | 1.8/3.5 |
| [21] | $29.6 \times 14.8 \times 1.5$ | 2.4 | 2.5/3.5 |
| [22] | $30 \times 40 \times 0.8$ | 5.2/5.8 | 2.3/3.5/5.5 |
| [23] | $50 \times 50 \times 1.6$ | 5.2/5.8 | 3.5 |
| [24] | $80 \times 60 \times 0.2$ | 2.4/3.65 | 2.3/2.5/3.5 |
| [25] | $35 \times 25 \times 1$ | 2.4/5.2/5.8 | 3.5/5.5 |
| [26] | $96 \times 73 \times 14$ | 2.4/5.2/5.8 | 2.5/3.5 |
| [27] | $24 \times 27 \times 1.6$ | 2.4/5.2/5.8 | 3.5 |
| [28] | $22 \times 29 \times 0.508$ | 2.4/5.2/5.8 | 3.5 |
| [29] | $35 \times 19 \times 1.6$ | 2.4/5.2/5.8 | 3.5/5.5 |
| [30] | $29 \times 21 \times 1.6$ | 2.4/5.2/5.8 | 3.5/5.5 |
| [31] | $50 \times 50 \times 1$ | 2.4/5.2/5.8 | 3.5/5.5 |
| Proposed | $17 \times 23.5 \times 1.6$ | 2.4/5.2/5.8 | 3.5/5.5 |

## 2. Antenna Structure

Figures 1(a) and 1(b) illustrate the top and side views of the WLAN/WiMAX triband compact printed antenna. The proposed antenna is mounted on the FR-4 substrate whose dielectric constant ($\varepsilon_r$), loss tangent ($\tan\delta$), and thickness ($h$) are 4.4, 0.02, and 1.6 mm, respectively. The overall size of the triband antenna is $17 \times 23.5 \times 1.6$ mm. The antenna structure consists of 50 Ω coplanar waveguide (CPW) feed, three radiating components (i.e., a folded open stub and long and short L-shaped strips), and asymmetric trapezoid ground plane.

The asymmetric trapezoid ground plane is incorporated to fine-tune impedance matching at 5.2, 5.5, and 5.8 GHz. Table 2 tabulates the optimal dimensions of the proposed WLAN/WiMAX triband compact printed antenna.

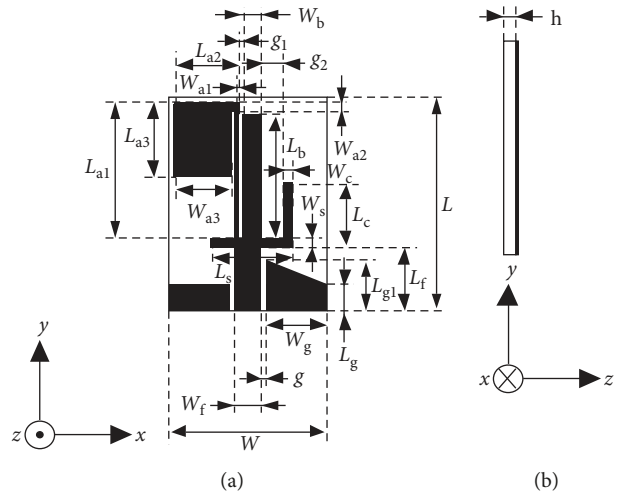


Figure 1: The proposed WLAN/WiMAX triband antenna: (a) top view and (b) side view.

## 3. Design Principle and Parametric Study

*3.1. Antenna Design Evolution.* In the antenna design evolution, simulations were carried out using CST software by varying dimensions of three radiating components, and the reflection coefficient ($|S_{11}|$) was determined. Figure 2 illustrates the evolution of the WLAN/WiMAX triband compact printed antenna. Specifically, in order to achieve the miniaturization of the antenna structure, the open stub in Antenna1 is folded. The folded open stub with coupling gap (Antenna1) was first realized to achieve dual resonant frequencies ($|S_{11}| < -10$ dB) at 2.4 and 5.8 GHz. A long strip was then introduced to form a long L-shaped strip (Antenna2) to generate resonance at 3.5 GHz WiMAX frequency. A short strip was next added to form a short L-shaped strip (Antenna3) to achieve the resonant frequency at 5.2 GHz. A triangular-shaped strip was incorporated into the existing ground plane to realize the asymmetric trapezoid ground plane (the proposed antenna) to fine-tune impedance matching at the upper frequency band, i.e., 5.2, 5.5, and 5.8 GHz.

Table 2: The optimal dimensions of the WLAN/WiMAX triband antenna (unit: mm).

| Parameter | $L$ | $W$ | $W_s$ | $W_{a1}$ | $W_{a2}$ | $W_{a3}$ | $W_b$ | $W_c$ | $g$ | $g_1$ | $g_2$ | $L_g$ | $L_{g1}$ | $L_f$ | $L_s$ | $L_{a1}$ | $L_{a2}$ | $L_{a3}$ | $L_b$ | $L_c$ |
|---|---|---|---|---|---|---|---|---|---|---|---|---|---|---|---|---|---|---|---|---|
| Dimension | 23.5 | 17 | 1 | 0.5 | 1.1 | 6.2 | 2.1 | 1.2 | 0.4 | 0.2 | 2.3 | 3 | 0.2 | 7 | 9 | 14.82 | 7.1 | 8.2 | 13.45 | 7 |

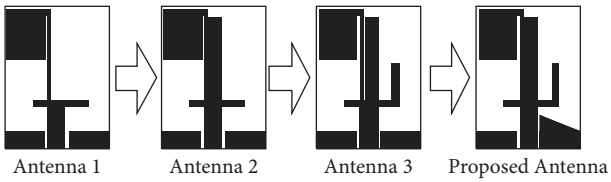


Figure 2: Evolution of the WLAN/WiMAX triband compact printed antenna.

In the parametric study of the antenna, the dimensions of a folded open stub, long and short L-shaped strips, and asymmetric trapezoid ground plane were varied and the reflection coefficient ($|S_{11}|$) was determined, as shown in Sections 3.2 and 3.3.

*3.2. Radiating Elements: Folded Open Stub, Long L-Shaped Strip, and Short L-Shaped Strip.* The basic structure of the proposed antenna consists of a folded open stub and long and short L-shaped strips, as shown in Figures 3(a)–3(c). Based on $|S_{11}| < -10$ dB criteria, Figures 4(a)–4(c), respectively, illustrate the simulated $|S_{11}|$ of Antenna1, Antenna2, and Antenna3. Figure 4(a) shows the simulated $|S_{11}|$ of Antenna1 (folded open stub) under variable folded open stub widths ($W_{a3}$): 4.4, 5.3, 6.2, and 7.1 mm. The folded open stub achieves two resonant frequencies, and both resonant frequencies shift to higher frequency bands as $W_{a3}$ increases. The result indicates that 6.2 mm is the optimal $W_{a3}$ because of resonance proximity to 2.4 GHz (2.417–2.576 GHz; first resonance at 2.496 GHz) and 5.8 GHz (5.483–6.362 GHz; second resonance at 5.808 GHz) WLAN bands.

In Figure 4(b), the length of the long L-shaped strip ($L_b$) in Antenna2 (folded open stub and long L-shaped strip components) is varied between 9.45, 11.45, 13.45, and 15.45 mm. The simulated $|S_{11}|$ indicates that the optimal $L_b$ is 13.45 mm with the resonant frequency at 3.496 GHz (3.356–3.663), near the 3.5 GHz WiMAX band. In Figure 4(c), the length of the short L-shaped strip ($L_c$) is varied between 5.84, 6.42, 7, and 7.58 mm. The simulated $|S_{11}|$ shows that, given $L_c = 7$ mm, Antenna3 (folded open stub and long and short L-shaped strips) realizes four resonances at 2.432, 3.496, 5.067, and 5.698 GHz, with the corresponding frequency bands of 2.387–2.474, 3.361–3.647, 4.884–5.332, and 5.467–6.060 GHz. The optimal $L_c$ is thus 7 mm, given the proximity of the 5.067 GHz resonant frequency to 5.2 GHz WLAN band.

In addition, the overall length of the folded open stub ($L_{a1} + L_{a2} + L_{a3}$) at 2.4 GHz WLAN frequency is about a quarter wavelength (31.25 mm). Besides, the coupling gap in the folded open stub enables frequency resonance at 5.8 GHz. Similarly, the overall length of the long L-shaped strip ($L_b + (L_s - W_c - g_2) + W_s$) at 3.5 GHz WiMAX frequency is approximately a quarter wavelength (21.43 mm). The entire length of the short L-shaped strip ($L_s + L_c$) at 5.2 GHz WLAN frequency is around a quarter wavelength (14.42 mm), as shown in Figures 3(a)–3(c).

*3.3. Trapezoid Ground Plane.* To improve impedance matching at the upper frequency band (i.e., 5.2, 5.5, and 5.8 GHz), a triangular-shaped strip was incorporated into the existing ground plane to realize the asymmetric trapezoid ground plane (proposed antenna), as shown in Figure 5(a). The slope of the triangular-shaped strip ($L_{g1}$) of the trapezoid ground plane is varied between 3, 4.3, 5.6, and 6.9 mm. The simulated $|S_{11}|$ shows that, given $L_{g1} = 5.6$ mm, the asymmetric trapezoid ground plane achieves four resonances and is able to fine-tune impedance matching in the 4.976–6.998 GHz frequency range, covering 2.397–2.485 GHz (first resonance at 2.440 GHz), 3.398–3.718 GHz (second resonance at 3.544 GHz), 4.976–6.998 GHz (third and fourth resonances at 5.226 GHz and 5.776 GHz), as shown in Figure 5(b).

*3.4. Input Impedance on the Smith Chart.* With the theoretical formulation of the input impedance characteristics, the expression for the input impedance of the CPW equivalent lossless transmission line can be expressed as [32]

$$Z_{in} = R_0 \left[ \frac{Z_L + jR_0 \tan(\beta l)}{R_0 + jZ_L \tan(\beta l)} \right], \quad (1)$$

where $Z_L$ is the input impedance of the antenna, $R_0$ is the characteristic impedance of the CPW transmission line, $\beta$ is the phase constant, and $l$ is the length of the transmission line.

The normalized input impedance on the Smith chart whose standing wave ratio (SWR) is 2 is equivalent to $|S_{11}| = -10$ dB. Figure 6(a) depicts the simulated $|S_{11}|$ at various stages of antenna evolution, from Antenna1, Antenna2, and Antenna3, to WLAN/WiMAX triband antenna.

In Figure 6(b), Antenna1 is operable in 2.417–2.576 and 5.483–6.362 GHz frequency bands, with the first and second resonances at 2.496 and 5.808 GHz, respectively, corresponding to Figure 6(a). In Figure 6(c), Antenna2 covers three frequency bands: 2.394–2.487 GHz (first resonance at 2.440 GHz), 3.356–3.663 GHz (second resonance at 3.496 GHz), and 5.534–6.334 GHz (third resonance at 5.768 GHz), corresponding to Figure 6(a).

In Figure 6(d), Antenna3 achieves four resonant frequencies: 2.432 GHz for 2.387–2.474 GHz frequency band, 3.496 GHz for 3.361–3.647 GHz band, 5.067 GHz for 4.884–5.332 GHz band, and 5.698 GHz for 5.467–6.060 GHz band, consistent with Figure 6(a). In Figure 6(e), the proposed WLAN/WiMAX triband antenna covers three frequency bands with four resonances: 2.397–2.485 GHz (first resonance at 2.440 GHz), 3.398–3.718 GHz (second resonance at 3.544 GHz), and 4.976–6.998 GHz (third and fourth

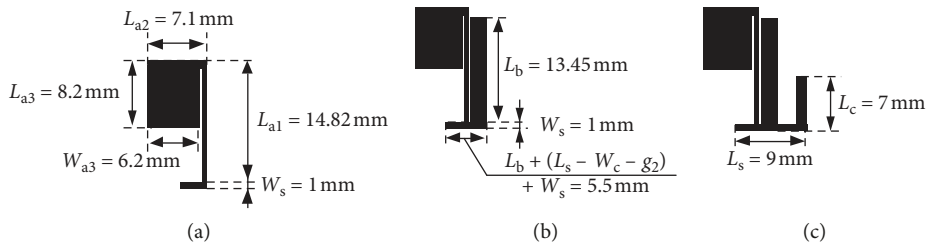


FIGURE 3: The radiating elements: (a) a folded open stub (Antenna1), (b) a folded open stub and a long L-shaped strip (Antenna2), (c) afolded open stub and long and short L-shaped strips (Antenna3).

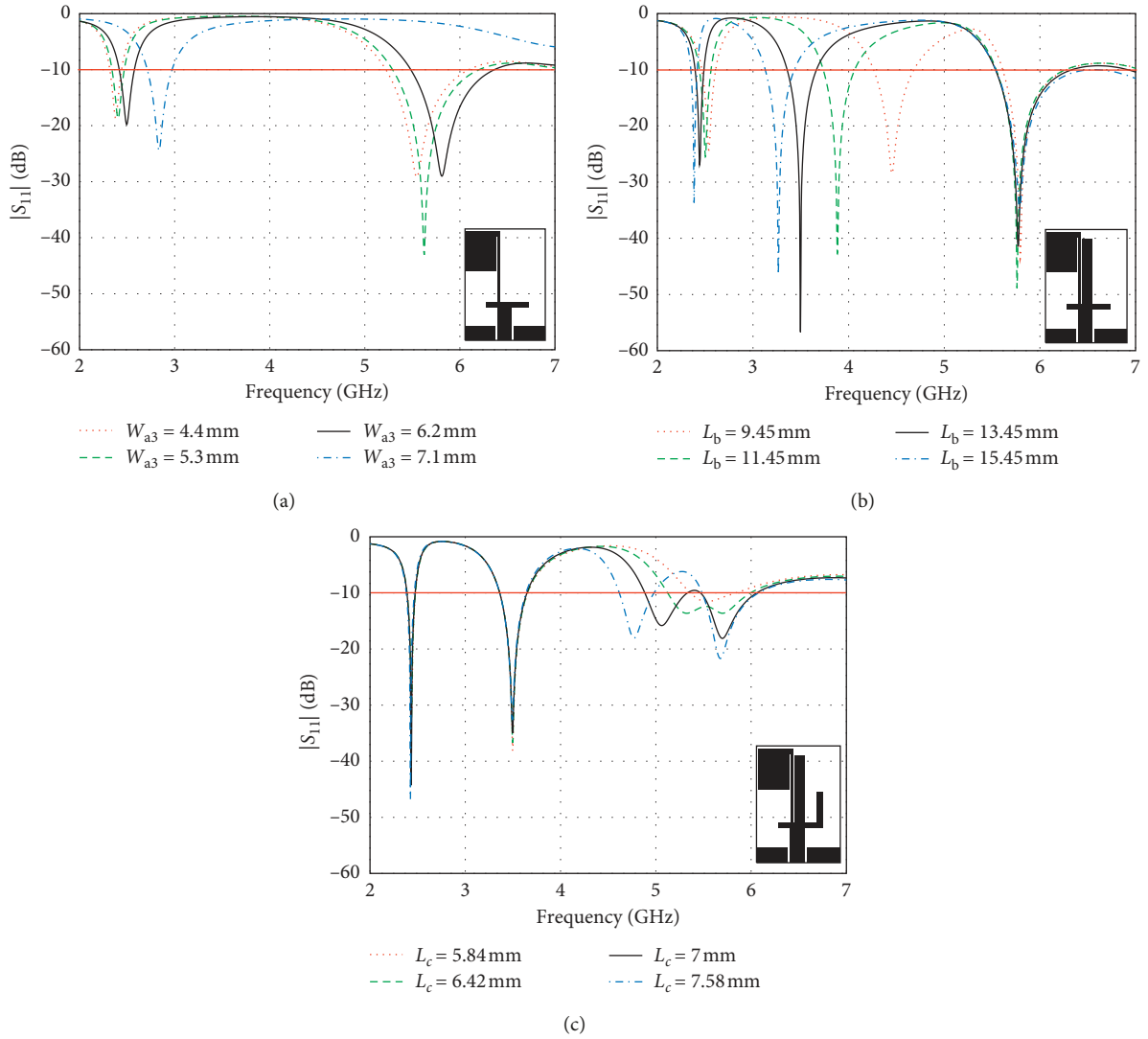


FIGURE 4: Simulated |$S_{11}$| at various stages of antenna evolution: (a) Antenna1, (b) Antenna2, and (c) Antenna3.

resonances at 5.226 and 5.776 GHz), thus covering 2.4/5.2/5.8 GHz WLAN and 3.5/5.5 GHz WiMAX bands.

*3.5. Equivalent Circuit Model.* The matching network topologies used in several antennas are equivalent circuit models [33–35]. For instance, the multi-input multi-output (MIMO) antenna system with nonresonant elements used LC components for matching the low- and high-frequency range [33], while the monopole antennas are designed as series or parallel RLC components or a combination of series and parallels, which are based on the CPW model [34, 35].

To discuss the relation between the triband frequency operation and input impedance properties of each antenna element, the equivalent circuit model is built, as shown in Figure 7. The corresponding equivalent circuit model

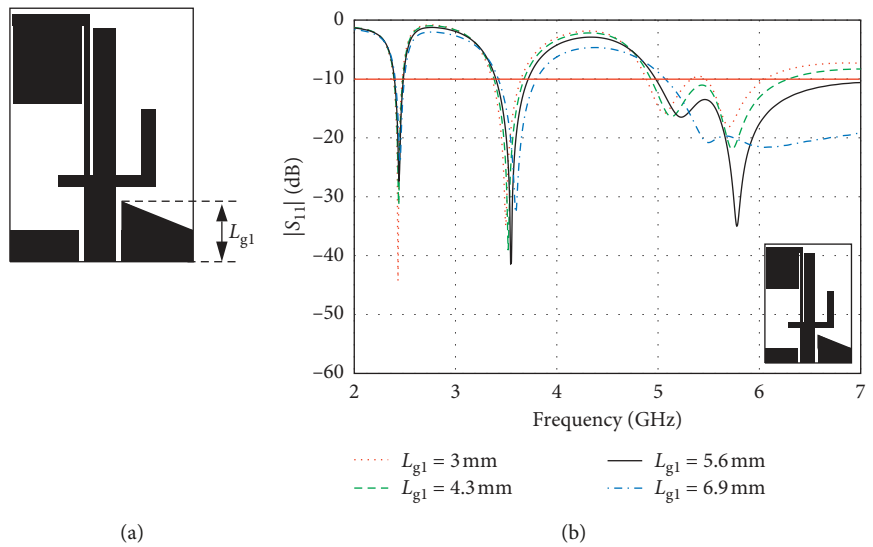


Figure 5: Simulated $|S_{11}|$ at various stages of antenna evolution: the proposed antenna.

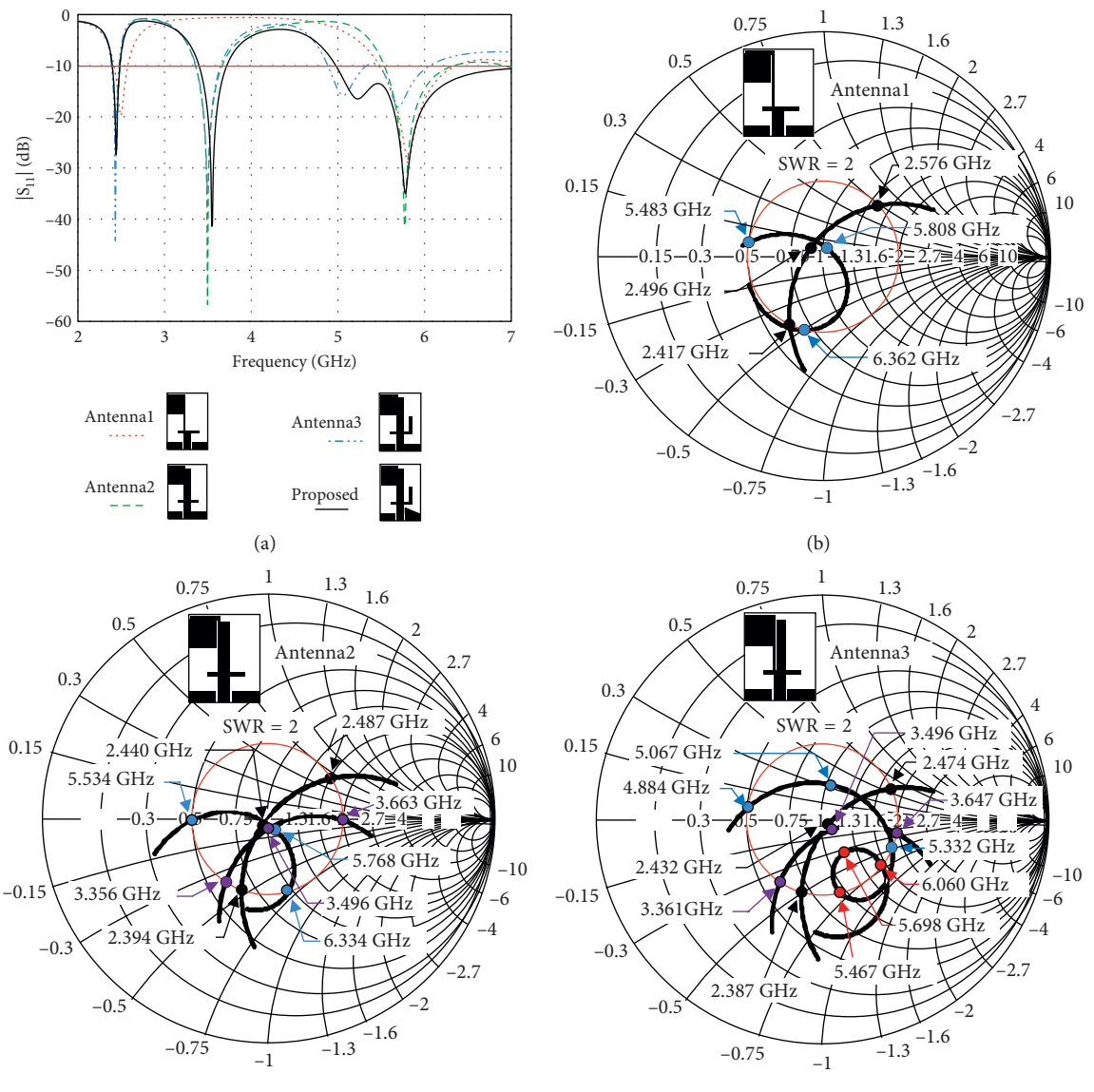


Figure 6: Continued.

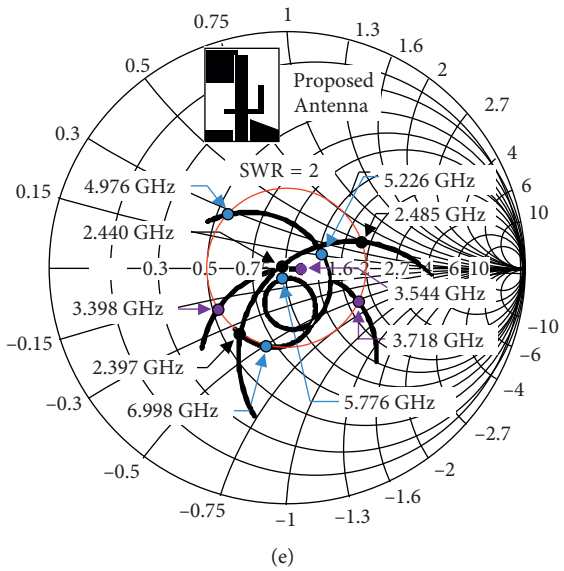


(e)

Figure 6: Comparison between the simulated $|S_{11}|$ and normalized input impedance at various stages of antenna evolution: (a) $|S_{11}|$, (b) Antenna1, (c) Antenna2, (d) Antenna3, and (e) the proposed antenna.

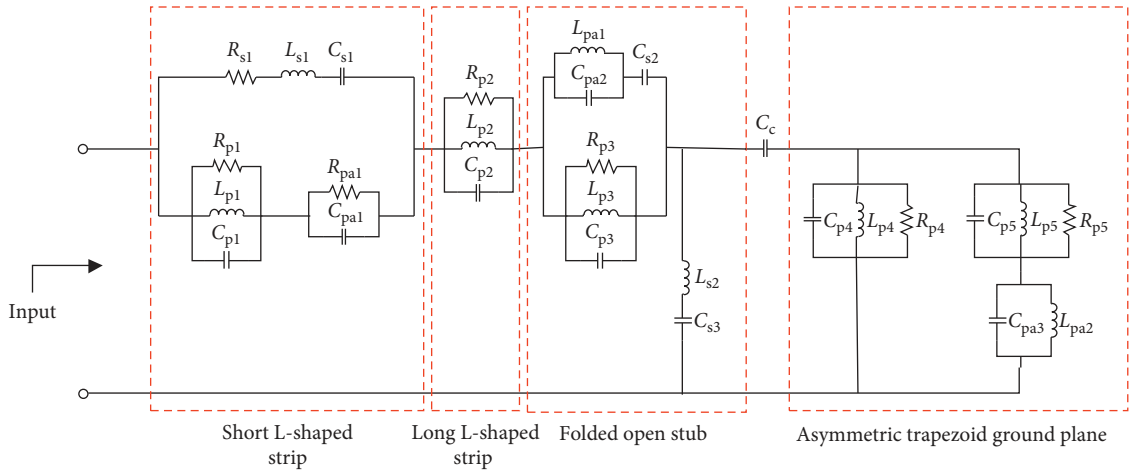


Figure 7: Equivalent circuit model of the WLAN/WiMAX triband compact printed antenna.

consists of a parallel RLC, series RLC, parallel LC, series LC, and parallel RC resonant circuit. The values of equivalent circuit elements can be calculated [36], and the optimized values will be subsequently determined.

The resonant frequency can be calculated using the following equation:

$$\omega_0 = \frac{1}{\sqrt{LC}}, \tag{2}$$

where the −3 dB bandwidth (BW) for the series resonant circuit is given by

$$\text{BW} = \frac{1}{Q} = 2\frac{\Delta\omega}{\omega_0} = \frac{R}{\omega_0 L}, \tag{3}$$

and the bandwidth for the parallel resonant circuit can be determined from

$$\text{BW} = \frac{1}{Q} = 2\frac{\Delta\omega}{\omega_0} = \frac{1}{\omega_0 RC}. \tag{4}$$

The initial values of $R$, $L$, and $C$ can be calculated by using (2)–(4). The equivalent circuit model is built, and the optimized values of lumped elements can be calculated using Agilent Advanced Design System (ADS) software package. Figure 7 illustrates the equivalent lumped-element electrical model of the proposed antenna consisting of four stages: first (short L-shaped strip) is connected with the second stage (long L-shaped strip) in series and the third stage (folded open stub), and then a coupling capacitor ($C_c$) is connected with the fourth stage (asymmetric trapezoid ground plane) in series.

In Figure 7, a series RLC ($R_{s1}$, $L_{s1}$, $C_{s1}$), a parallel RLC ($R_{p1}$, $L_{p1}$, $C_{p1}$), and a parallel RC ($R_{pa1}$, $C_{pa1}$) are connected in parallel at the first stage, which are responsible for generating the current mainly flowing along a short L-shaped strip, in which the parallel and series resonant circuits will achieve the resonant frequency at 5.2 GHz, corresponding to the surface current distribution shown in Figure 8(c).

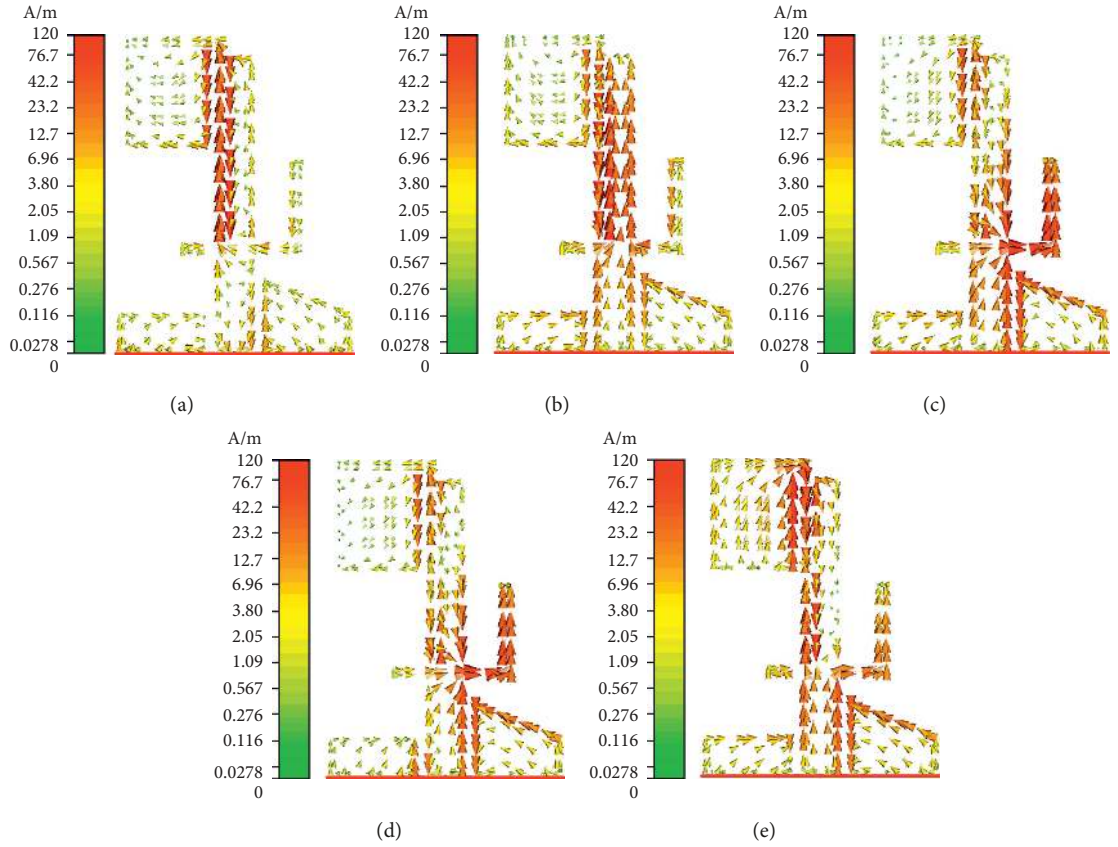


Figure 8: Simulated surface current distribution of the WLAN/WiMAX triband antenna at (a) 2.4, (b) 3.5, (c) 5.2, (d) 5.5, and (e) 5.8 GHz.

At the second stage, a parallel RLC ($R_{p2}$, $L_{p2}$, $C_{p2}$) is connected in series with the first stage, for producing the current along a long L-shaped strip, in which the parallel and series resonant circuits will achieve the resonant frequency at 3.5 GHz, corresponding to the surface current distribution shown in Figure 8(b).

At the third stage, a parallel RLC resonant circuit ($R_{p3}$, $L_{p3}$, $C_{p3}$) is in parallel with a combination of a parallel LC ($L_{pa1}$, $C_{pa2}$) and a series capacitor ($C_{s2}$). Then, this circuit is connected with a series LC ($L_{s2}$, $C_{s3}$) for creating the current flowing along the folded open stub. These parallel and series resonant circuits yield the resonant frequency at 2.4 and 5.8 GHz, corresponding to the surface current distribution in Figures 8(a) and 8(e).

In addition, at the fourth stage (asymmetric trapezoid ground plane), a coupling capacitor ($C_c$) is connected in series with a parallel RLC ($R_{p4}$, $L_{p4}$, $C_{p4}$) and a parallel RLC ($R_{p5}$, $L_{p5}$, $C_{p5}$) with a parallel LC circuit ($L_{pa2}$, $C_{pa3}$), corresponding to the surface current concentrated along the edge of the trapezoid ground plane at the frequency of 5.2, 5.5, and 5.8 GHz as shown in Figures 8(c)–8(e), respectively. The optimized lumped-element values are given in Table 3.

In Figures 9(a)–9(c), the CST simulated and calculated input impedance and $|S_{11}|$ of the equivalent lumped-element circuit are compared. The result shows that the CST simulations and calculations of the equivalent circuit are in good agreement. In particular, $|S_{11}|$ is identical to the resonance existing between the two curves as shown in Figure 9(c).

*3.6. Current Distribution.* Figures 8(a)–8(e), respectively, illustrate the CST simulated surface current distribution of the WLAN/WiMAX triband compact printed antenna at 2.4, 3.5, 5.2, 5.5, and 5.8 GHz. The results reveal that, at 2.4 and 5.8 GHz, the surface current is concentrated along the folded open stub. At 3.5 GHz, the surface current is concentrated on the long L-shaped strip, while the concentration of surface current is noticeably high on the short L-shaped strip at 5.2 GHz. At 5.5 GHz, the surface current is concentrated around the folded open stub and short L-shaped strip.

In particular, at 5.2, 5.5, and 5.8 GHz, the surface current is concentrated along the edge of the trapezoid ground plane, thereby fine-tuning impedance matching of the upper frequency bands. In essence, the triband characteristic of the antenna is a collective function of the folded open stub, long and short L-shaped strips, and asymmetric trapezoid ground plane.

## 4. Results and Discussion

A prototype of the WLAN/WiMAX triband compact printed antenna was fabricated, as shown inFigure10, and experiments were then carried out. Figure 11 compares the

Table 3: The optimal component values of an equivalent circuit model of the proposed antenna.

| Lumped element | Value |
|---|---|
| $R_{p1}$ | 32 Ω |
| $L_{p1}$ | 0.17 nH |
| $C_{p1}$ | 4.7 pF |
| $R_{s1}$ | 12 Ω |
| $L_{s1}$ | 1.5 nH |
| $C_{s1}$ | 2 pF |
| $R_{p2}$ | 49 Ω |
| $L_{p2}$ | 0.39 nH |
| $C_{p2}$ | 5.36 pF |
| $R_{pa1}$ | 32 Ω |
| $C_{pa1}$ | 12 pF |
| $L_{pa1}$ | 0.23 nH |
| $C_{pa2}$ | 5 pF |
| $R_{p3}$ | 28.5 Ω |
| $L_{p3}$ | 0.18 nH |
| $C_{p3}$ | 4.7 pF |
| $L_{pa1}$ | 0.23 nH |
| $C_{pa2}$ | 2 pF |
| $C_{s2}$ | 7.8 pF |
| $L_{s2}$ | 0.8 nH |
| $C_{s3}$ | 4.2 pF |
| $C_c$ | 200 nF |
| $R_{p4}$ | 36 Ω |
| $L_{p4}$ | 2.8 nH |
| $C_{p4}$ | 0.25 pF |
| $R_{p5}$ | 49 Ω |
| $L_{p5}$ | 0.15 nH |
| $C_{p5}$ | 4.2 pF |
| $C_{pa3}$ | 10.27 pF |
| $L_{pa2}$ | 0.0775 nH |

simulated and experimental $|S_{11}|$ of the proposed triband antenna relative to frequency, using an Agilent HP8720C vector network analyzer. The antenna prototype achieves triple frequency bands: 2.29–2.59 GHz, 3.37–3.75 GHz, and 4.85–6.23 GHz, with $|S_{11}| < -10$ dB. In the figure, the simulated and measured results are in good agreement.

Figures 12(a)–12(e), respectively, illustrate the far-field simulated and measured radiation patterns at 2.4, 3.5, 5.2, 5.5, and 5.8 GHz. The simulated and measured co-polarized (co-pol) radiation patterns in the *xz* (azimuth plane) and *yz* planes (elevation plane) are omnidirectional at 2.4, 3.5, and 5.2 GHz and near-omnidirectional at 5.5 and 5.8 GHz. The simulated and measured results are in good agreement. The differences between the simulated co-polarization and cross polarization (x-pol) in the *xz* plane are 9, 22, 5, 10, and 13 dB at 2.4, 3.5, 5.2, 5.5, and 5.8 GHz, respectively, which is due mainly to an asymmetric structure of the antenna. However, the cross-polarization level is 22 dB relatively lower than the co-polarization level at 3.5 GHz.

Figures 13(a)–13(e) illustrate the simulated and measured gains of the WLAN/WiMAX triband compact printed antenna at 2.4, 3.5, 5.2, 5.5, and 5.8 GHz, respectively, and Table 4 compares the simulated and measured antenna gains. The results show good agreement between simulated and measured results. However, there

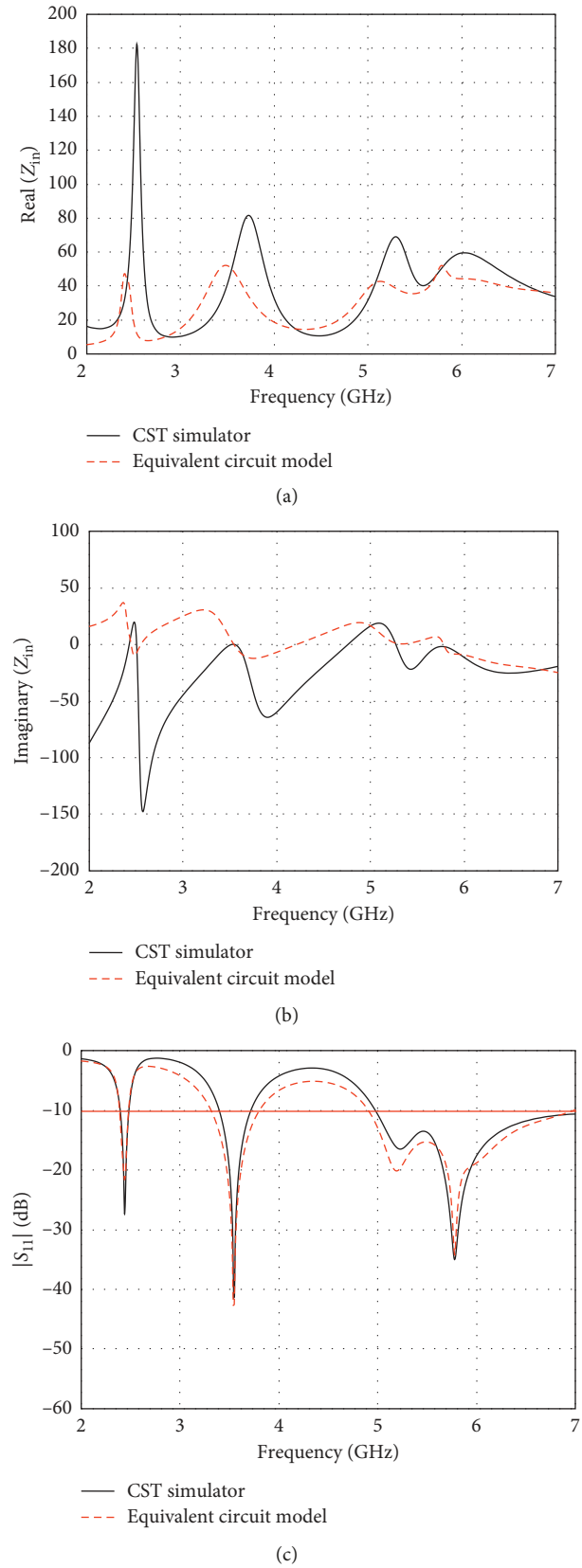


Figure 9: Comparison between the simulated input impedance and $|S_{11}|$ of the proposed antenna by CST and the equivalent circuit model:(a) impedance real part; (b) impedance imaginary part; (c) $|S_{11}|$.

Figure 10: Prototype of the WLAN/WiMAX triband antenna.

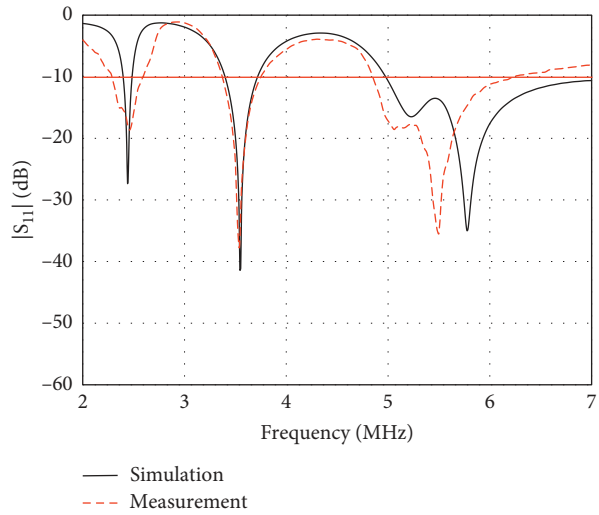


Figure 11: Simulated and measured $|S_{11}|$ of the triband antenna.

exist small discrepancies between the simulated and measured antenna gains, which is attributable to fabrication tolerance, experimental setting, and antenna material losses.

## 5. Conclusion

This research proposed a WLAN/WiMAX triband compact printed antenna using a folded open stub, long and short L-shaped strips, and asymmetric trapezoid ground plane. The triband antenna is of simple structure and operable in 2.4 GHz, 5 GHz (5.2/5.8 GHz) WLAN and 3.5/5.5 GHz WiMAX bands. The folded open stub achieves resonant frequencies at 2.4 and 5.8 GHz, and the long and short L-shaped strips at 3.5 GHz and 5.2 GHz, respectively. The asymmetric trapezoid ground plane is incorporated to fine-tune impedance matching at 5.2, 5.5, and 5.8 GHz. The equivalent lumped-element circuit of

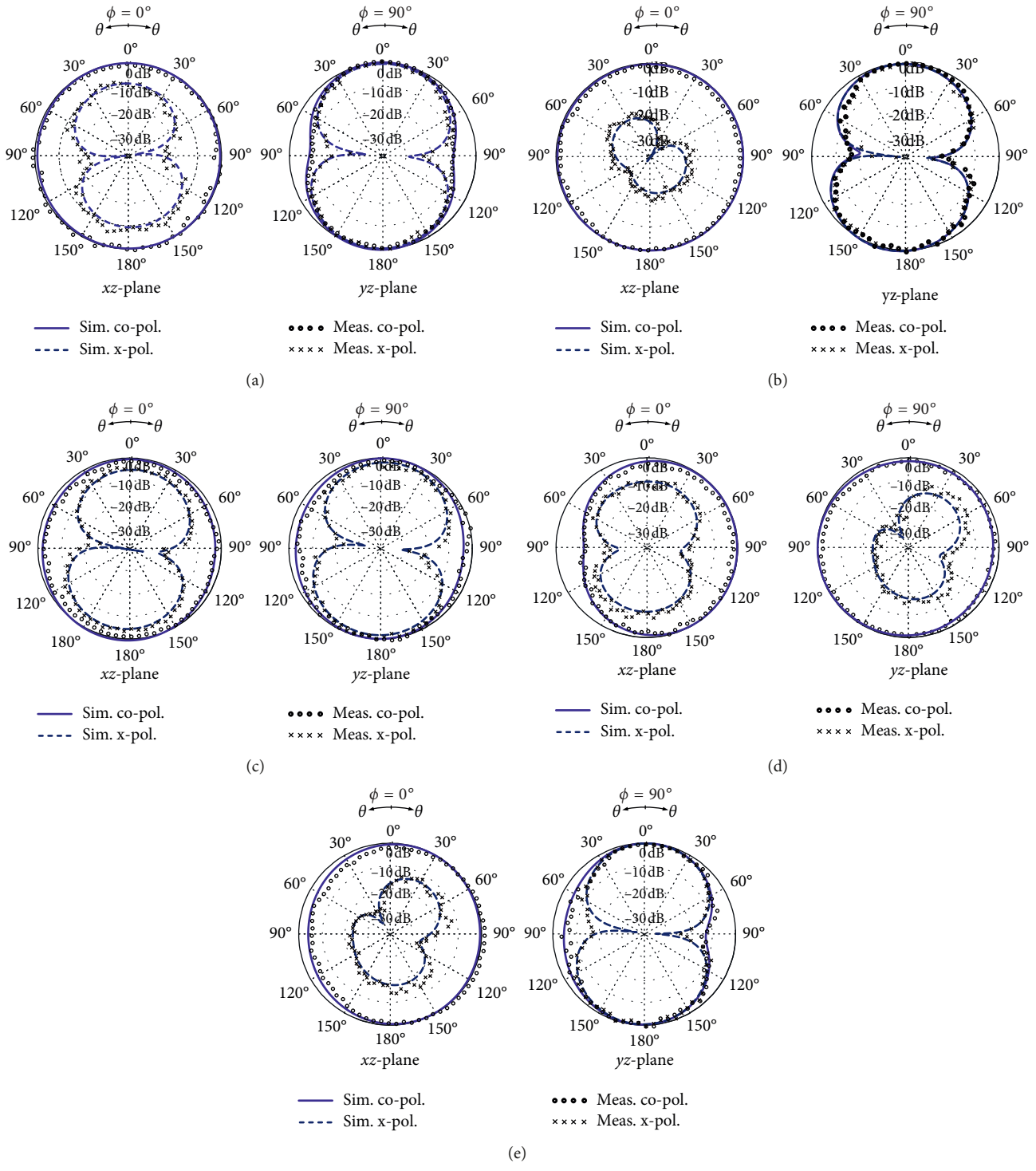


Figure 12: Simulated and measured radiation pattern of the WLAN/WiMAX triband antenna at (a) 2.4, (b) 3.5, (c) 5.2, (d) 5.5, and (e) 5.8 GHz.

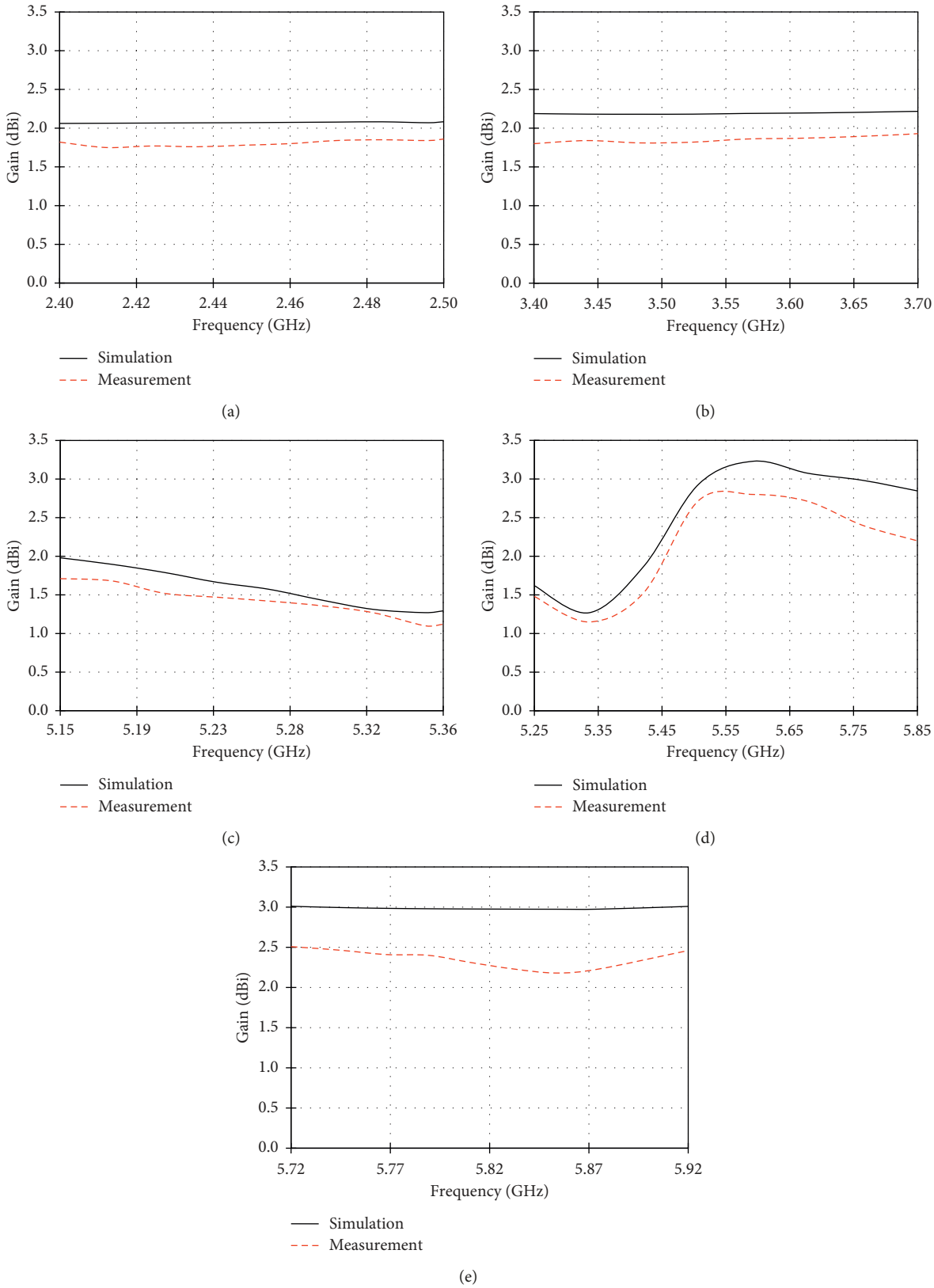


Figure 13: Simulated and measured gain of the WLAN/WiMAX triband antenna at (a) 2.4, (b) 3.5, (c) 5.2, (d) 5.5, (e) and 5.8 GHz.

Table 4: Simulated and measured antenna gains.

| Frequency | 2.4 GHz (2.4–2.484 GHz) | 3.5 GHz (3.4–3.6 GHz) | 5.2 GHz (5.15–5.35 GHz) | 5.5 GHz (5.25–5.85 GHz) | 5.8 GHz (5.725–5.825 GHz) |
|---|---|---|---|---|---|
| Simulated | 2.059–2.078 dBi | 2.180–2.215 dBi | 1.270–1.980 dBi | 1.269–3.074 dBi | 2.974–3.007 dBi |
| Min. | 2.059 dBi at 2.4 GHz | 2.180 dBi at 3.48 GHz | 1.270 dBi at 5.35 GHz | 1.269 dBi at 5.34 GHz | 2.974 dBi at 5.811 GHz |
| Max. | 2.078 dBi at 2.484 GHz | 2.195 dBi at 3.6 GHz | 1.980 dBi at 5.15 GHz | 3.074 dBi at 5.68 GHz | 3.007 dBi at 5.725 GHz |
| Measured | 1.75–1.85 dBi | 1.80–1.92 dBi | 1.10–1.71 dBi | 1.15–2.80 dBi | 2.18–2.18 dBi |
| Min. | 1.75 dBi at 2.41 GHz | 1.80 dBi at 3.40 GHz | 1.10 dBi at 5.35 GHz | 1.15 dBi at 5.34 GHz | 2.23 dBi at 5.82 GHz |
| Max. | 1.85 dBi at 2.48 GHz | 1.87 dBi at 3.60 GHz | 1.71 dBi at 5.15 GHz | 2.80 dBi at 5.59 GHz | 2.50 dBi at 5.73 GHz |

the proposed antenna was also studied and validated, which exhibits triband resonant characteristics. Simulations were carried out, an antenna prototype fabricated, and experiments undertaken. The simulated and experimental far-field radiation pattern of the triband antenna is omnidirectional at 2.4, 3.5, and 5.2 GHz and near-omnidirectional at 5.5 and 5.8 GHz. The simulated and measured antenna gains are 1.269–3.074 dBi and 1.10–2.80 dBi, respectively. The simulation and experimental results are in good agreement. Essentially, the proposed triband compact printed antenna covers 2.4 GHz, 5 GHz (5.2/5.8 GHz) WLAN, and (3.5/5.5 GHz) WiMAX frequency bands and therefore possesses high potential for WLAN/WiMAX applications.

## Data Availability

The data used to support the findings of this study are available from the corresponding author upon request.

## Conflicts of Interest

The authors declare that they have no conflicts of interest.

## Acknowledgments

This work has been supported by the Thailand Research Fund through the TRF Senior Research Scholar Program with Grant no. RTA6080008. The authors would like to express their deep gratitude to the Faculty of Technical Education, Rajamangala University of Technology Isan Khonkaen Campus, and to the Antenna and Electromagnetic Applications Research Laboratory, King Mongkut's Institute of Technology Ladkrabang, Bangkok, Thailand.

## References

[1] C.-T. Lee and S.-W. Su, "Very-low-profile, 2.4/5.2/5.8-GHz, triband WLAN antenna for laptop-tablet computer with complete metal cover," *Microwave and Optical Technology Letters*, vol. 58, no. 1, pp. 225–233, 2016.

[2] W. Chen, F. Li, M. Li, J. Yang, and J. Yin, "Directional dual-band slotted semi-circular inverted-F antenna for WLAN applications," *Electronics Letters*, vol. 51, no. 24, pp. 1960–1962, 2015.

[3] G. A. Casula, G. Montisci, P. Maxia, G. Valente, A. Fanti, and G. Mazzarella, "A low-cost dual-band CPW-fed printed LPDA for wireless communications," *IEEE Antennas and Wireless Propagation Letters*, vol. 15, pp. 1333–1336, 2016.

[4] C.-Y.-D. Sim, C.-C. Chen, X. Y. Zhang, Y.-L. Lee, and C.-Y. Chiang, "Very small-size uniplanar printed monopole antenna for dual-band WLAN laptop computer applications," *IEEE Transactions on Antennas and Propagation*, vol. 65, no. 6, pp. 2916–2922, 2017.

[5] C.-T. Lee, S.-W. Su, S.-C. Chen, and C.-S. Fu, "Low-cost, direct-fed slot antenna built in metal cover of notebook computer for 2.4-/5.2-/5.8-GHz WLAN operation," *IEEE Transactions on Antennas and Propagation*, vol. 65, no. 5, pp. 2677–2682, 2017.

[6] A. K. Sharma, B. V. R. Reddy, and A. Mittal, "Slot embedded dual-band patch antenna for WLAN and WiMAX applications," *Electronics Letters*, vol. 51, no. 8, pp. 608-609, 2015.

[7] K.-H. Chen, Y.-C. Lo, Y.-S. Lee, S.-J. Wu, and J.-H. Tarng, "Compact four bands hybrid filtering antenna using step impedance resonators and tuning stub transition structures," *IET Microwaves, Antennas & Propagation*, vol. 12, no. 7, pp. 1126–1131, 2018.

[8] A. Sharma, P. Ranjan, and R. K. Gangwar, "Multiband cylindrical dielectric resonator antenna for WLAN/WiMAX application," *Electronics Letters*, vol. 53, no. 3, pp. 132–134, 2017.

[9] S. C. Basran, U. Olgun, and K. Sertel, "Multiband monopole antenna with complementary split-ring resonators for WLAN and WiMAX applications," *Electronics Letters*, vol. 49, no. 10, pp. 636–638, 2013.

[10] A. Kumar, J. K. Deegwal, and M. M. Sharma, "Design of multi-polarised quad-band planar antenna with parasitic multistubs for multiband wireless communication," *IET Microwaves, Antennas & Propagation*, vol. 12, no. 5, pp. 718–726, 2018.

[11] S. Mathew, M. P. Jayakrishnan, K. Vasudevan, M. Ameen, and P. Mohanan, "Compact dual polarised V slit, stub and slot embedded circular patch antenna for UMTS/WiMAX-WLAN applications," *Electronics Letters*, vol. 52, no. 17, pp. 1452–1426, 2016.

[12] T. Wu, X.-W. Shi, H. Bai, and P. Li, "Tri-band microstrip-fed monopole antenna with dual-polarisation characteristics for WLAN and WiMAX applications," *Electronics Letters*, vol. 49, no. 25, pp. 1597-1598, 2013.

[13] C.-Y. Shual and G.-M. Wang, "A novel planar printed dual-band magneto-electric dipole antenna," *IEEE Access*, vol. 5, pp. 10062–10067, 2017.

[14] A. Boukarkar, X. Q. Lin, and Y. Jiang, "A dual-band frequency-tunable magnetic dipole antenna for WiMAX/WLAN applications," *IEEE Antennas and Wireless Propagation Letters*, vol. 15, pp. 492–495, 2016.

[15] S. Pandit, A. Mohan, and P. Ray, "Compact frequency-reconfigurable MIMO antenna for microwave sensing applications in WLAN and WiMAX frequency bands," *IEEE Sensors Letters*, vol. 2, no. 2, pp. 1–4, 2018.

[16] Y. I. Abdulraheem, G. A. Oguntala, A. S. Abdullah et al., "Design of frequency reconfigurable multiband compact antenna using two PIN diodes for WLAN/WiMAX applications," *IET Microwaves, Antennas & Propagation*, vol. 11, no. 8, pp. 1098–1105, 2017.

[17] S. M. Saeed, C. A. Balanis, and C. R. Birtcher, "Inkjet-printed flexible reconfigurable antenna for conformal WLAN/WiMAX wireless devices," *IEEE Antennas and Wireless Propagation Letters*, vol. 15, pp. 1979–1982, 2016.

[18] T. Li, H. Zhai, X. Wang, L. Li, and C. Liang, "Frequency-reconfigurable bow-tie antenna for bluetooth, WiMAX, and WLAN applications," *IEEE Antennas and Wireless Propagation Letters*, vol. 14, pp. 171–174, 2015.

[19] H. Li, Q. Zheng, J. Ding, and C. Guo, "Dual-band planar antenna loaded with CRLH unit cell for WLAN/WiMAX application," *IET Microwaves, Antennas & Propagation*, vol. 12, no. 1, pp. 132–136, 2018.

[20] C. Zhu, T. Li, K. Li et al., "Electrically small metamaterial-inspired tri-band antenna with meta-mode," *IEEE Antennas and Wireless Propagation Letters*, vol. 14, pp. 1738–1741, 2015.

[21] C. Zhou, G. Wang, J. Liang, Y. Wang, and B. Zong, "Broadband antenna employing simplified MTLs for WLAN/WiMAX applications," *IEEE Antennas and Wireless Propagation Letters*, vol. 13, pp. 595–598, 2014.

[22] S. Verma and P. Kumar, "Compact triple-band antenna for WiMAX and WLAN applications," *Electronics Letters*, vol. 50, no. 7, pp. 484–486, 2014.

[23] P. Surendrakumar and B. Chandra Mohan, "A triple-frequency, vertex-fed antenna for WLAN\/WiMAX applications [antenna applications corner]," *IEEE Antennas and Propagation Magazine*, vol. 60, no. 3, pp. 101–106, 2018.

[24] M. O. Sallam, S. M. Kandil, V. Volski, G. A. E. Vandenbosch, and E. A. Soliman, "Wideband CPW-fed flexible bow-tie slot antenna for WLAN/WiMAX systems," *IEEE Transactions on Antennas and Propagation*, vol. 65, no. 8, pp. 4274–4277, 2017.

[25] Y. Xu, Y.-C. Jiao, and Y.-C. Luan, "Compact CPW-fed printed monpole antenna with triple-band characteristics for WLAN/WiMAX applications," *Electronics Letters*, vol. 48, no. 24, pp. 1519-1520, 2012.

[26] M. van Rooyen, J. W. Odendaal, and J. Joubert, "High-gain directional anteanna for WLAN and WiMAX applications," *IEEE Antennas and Wireless Propagation Letters*, vol. 16, pp. 286–289, 2017.

[27] P. S. Bakariya, S. Dwari, M. Sarkar, M. K. Mandal, and R. Nicole, "Proximity-coupled microstrip antenna for bluetooth, WiMAX, and WLAN applications," *IEEE Antennas and Wireless Propagation Letters*, vol. 14, pp. 755–758, 2015.

[28] A. Mehdipour, A. R. Sebak, C. W. Trueman, and T. A. Denidni, "Compact multiband planar antenna for 2.4/3.5/5.2/5.8-GHz wireless applications," *IEEE Antennas and Wireless Propagation Letters*, vol. 11, pp. 144–147, 2012.

[29] B. Li, Z.-H. Yan, and T.-L. Zhang, "Triple-band slot antenna with U-shaped open stub fed by asymmetric coplanar strip for WLAN/WiMAX applications," *Progress in Electromagnetics Research Letters*, vol. 37, pp. 123–131, 2013.

[30] H. Chen, X. Yang, Y. Z. Yin, S. T. Fan, and J. J. Wu, "Triband planar monopole antenna with compact radiator for WLAN/WiMAX applications," *IEEE Antennas and Wireless Propagation Letters*, vol. 12, pp. 1440–1443, 2013.

[31] F. Liu, K. Xu, P. Zhao, L. Dong, and G. Wang, "Uniplanar dual-band printed compound loop antenna for WLAN/WiMAX applications," *Electronics Letters*, vol. 53, no. 16, pp. 1083-1084, 2017.

[32] J. D. Kraus, *Antennas*, McGrew-Hill, New York, NY, USA, 2nd edition, 1997.

[33] A. Andujar and J. Anguera, "MIMO multiband antenna system with nonresonant elements," *Microwave and Optical Technology Letters*, vol. 57, no. 1, pp. 183–189, 2015.

[34] G. Tzeremes, T. S. Liao, P. K. L. Yu, and C. G. Christodoulou, "Computation of equivalent circuit models of optically driven CPW-fed slot antennas for wireless communications," *IEEE Antennas and Wireless Propagation Letters*, vol. 2, pp. 140–142, 2003.

[35] W.-C. Liu, "A coplanar waveguide-fed folded-slot monopole antenna for 5.8 GHz radio frequency identification application," *Microwave and Optical Technology Letters*, vol. 49, no. 1, pp. 71–74, 2007.

[36] X. Yang, F. Kong, X. Liu, and C. Song, "A CPW-fed triple-band antenna for WLAN and WiMAX applications," *Radio Engineering*, vol. 23, no. 4, pp. 1086–1091, 2014.